Title

Urbanization causes increased cloud base height and decreased fog in coastal Southern California

Journal

Geophysical Research Letters, 42(5)

ISSN

0094-8276

Authors

Williams, A Park
Schwartz, Rachel E
Iacobellis, Sam
et al.

Publication Date

2015-03-16

DOI

10.1002/2015gl063266

Peer reviewed

AGU PUBLICATIONS

Geophysical Research Letters

RESEARCH LETTER
10.1002/2015GL063266

Key Points:
- Low clouds regulate temperature and drought in coastal Southern California
- Urban warming has caused substantially increased cloud base height since 1948
- Feedbacks between warming and decreased summer cloud frequency are expected

Supporting Information:
- Tables S1–S4 and Figures S1–S6

Correspondence to:
A. P. Williams,
williams@ldeo.columbia.edu

Citation:
Williams, A. P., R. E. Schwartz, S. Iacobellis, R. Seager, B. I. Cook, C. J. Still, G. Husak, and J. Michaelsen (2015), Urbanization causes increased cloud base height and decreased fog in coastal Southern California, *Geophys. Res. Lett.*, *42*, 1527–1536, doi:10.1002/2015GL063266.

Received 26 JAN 2015
Accepted 18 FEB 2015
Accepted article online 20 FEB 2015
Published online 12 MAR 2015

Urbanization causes increased cloud base height and decreased fog in coastal Southern California

A. Park Williams[1], Rachel E. Schwartz[2], Sam Iacobellis[2], Richard Seager[1], Benjamin I. Cook[1,3], Christopher J. Still[4], Gregory Husak[5], and Joel Michaelsen[5]

[1]Lamont-Doherty Earth Observatory of Columbia University, Palisades, New York, USA, [2]Scripps Institution of Oceanography, University of California, San Diego, La Jolla, California, USA, [3]NASA Goddard Institute for Space Studies, New York, New York, USA, [4]Forest Ecosystems and Society, Oregon State University, Corvallis, Oregon, USA, [5]Geography Department, University of California, Santa Barbara, California, USA

Abstract Subtropical marine stratus clouds regulate coastal and global climate, but future trends in these clouds are uncertain. In coastal Southern California (CSCA), interannual variations in summer stratus cloud occurrence are spatially coherent across 24 airfields and dictated by positive relationships with stability above the marine boundary layer (MBL) and MBL height. Trends, however, have been spatially variable since records began in the mid-1900s due to differences in nighttime warming. Among CSCA airfields, differences in nighttime warming, but not daytime warming, are strongly and positively related to fraction of nearby urban cover, consistent with an urban heat island effect. Nighttime warming raises the near-surface dew point depression, which lifts the altitude of condensation and cloud base height, thereby reducing fog frequency. Continued urban warming, rising cloud base heights, and associated effects on energy and water balance would profoundly impact ecological and human systems in highly populated and ecologically diverse CSCA.

1. Introduction

Coastal Southern California (CSCA) is home to tens of millions of people and known globally for its mild climate. Summers in CSCA are generally cool and dry because high atmospheric pressure over the North Pacific Ocean promotes wind-driven upwelling of cold water and subsidence of warm, dry air from high above. The sinking air traps cool humid air within a thin marine boundary layer (MBL). Low stratus clouds within the MBL regulate radiation balance and surface temperature by shading during the day and trapping long-wave radiation at night [*Iacobellis and Cayan*, 2013]. Like the coast redwood trees further north [*Dawson*, 1998; *Johnstone and Dawson*, 2010], pine forests endemic to CSCA and Baja California respond positively to direct water deposition and shading from stratus clouds [*Baguskas et al.,* 2014; *Fischer et al.,* 2009; *Williams et al.,* 2008]. Coastal stratus and ground-level fog also influence grass and shrub species [*Corbin et al.,* 2005; *Vasey et al.,* 2012], streamflow [*Sawaske and Freyberg*, 2014], and soil respiration [*Carbone et al.,* 2013]. Stratus clouds also affect human systems. A change in daytime stratus frequency and shading would alter temperature, thereby affecting energy demand and public health [e.g., *Akbari et al.,* 2001; *Knowlton et al.,* 2009], but would oppositely affect solar energy harvesting and transportation safety. Effects of stratus on natural and human systems may converge via wildfire. Fog drip and cloud shading both regulate ecosystem water balance and atmospheric vapor-pressure deficit, key controls on wildfire risk [e.g., *Williams et al.,* 2015]. The broad impacts of stratus clouds and fog underlie concerns regarding how coastal stratus regimes may be altered in coming decades [e.g., *Johnstone and Dawson*, 2010; *Torregrosa et al.,* 2014].

Globally, subtropical stratus clouds are important regulators of radiation [*Hartmann et al.,* 1992; *Wood*, 2012], and even small changes to these clouds would have substantial feedbacks [*Webb et al.,* 2006]. Global climate models (GCMs) have difficulty accurately simulating low-level cloud processes [*Huang et al.,* 2013; *Lauer et al.,* 2010]. Differences in how these clouds are parameterized account for much of the intermodel spread among projections of global temperature [*Webb et al.,* 2013; *Soden and Vecchi*, 2011]. Even within high-resolution regional climate models, the many parameterization choices and their coupled effects contribute uncertainty to simulations of low marine clouds [*Huang et al.,* 2013], but recent efforts show promise [e.g., *O'Brien et al.,* 2013].

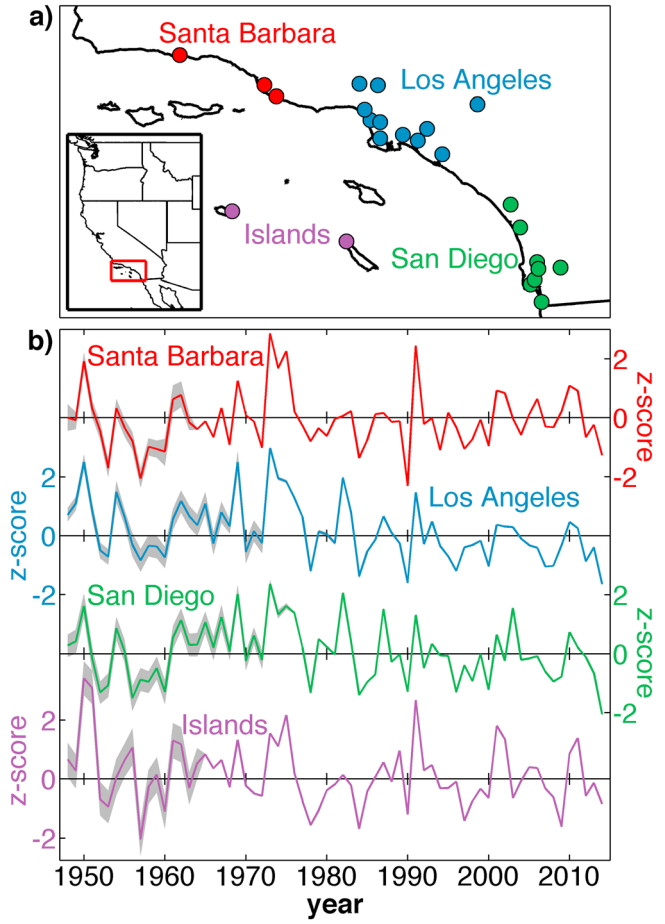

Figure 1. (a) Airfield locations and (b) time series of subregionally averaged May–September stratus frequency standardized to the 1973–2014 period. Colors of dots (Figure 1a) and line colors (Figure 1b) correspond to subregions. Grey shading around time series in Figure 1b bounds the 95% confidence interval. Inset in Figure 1a bounds the study region with a red box.

In light of modeling difficulties, it is particularly important to empirically diagnose variability and trends within observed cloud cover records [e.g., *Clement et al.*, 2009]. Using satellite observations of cloud cover over CSCA, *Iacobellis and Cayan* [2013] showed that stratus occurrence over the ocean and immediate CSCA coastline is closely tied to atmospheric stability above the MBL, which is promoted by cold sea surface temperatures (SSTs). Stratus occurrence over more inland areas, on the other hand, correlates with MBL depth. Further complexity is introduced by the combined findings of two recent investigations of trends since 1950. *Schwartz et al.* [2014] indicated only marginal declines in overall stratus occurrence at coastal airfields in Los Angeles, California, associated with a positive trend in the Pacific Decadal Oscillation, but other authors [*LaDochy*, 2005; *LaDochy and Witiw*, 2012; *Witiw and LaDochy*, 2008] indicate a near disappearance of ground-level fog during this period, suggesting a potential increase in cloud base height. Here we use hourly observations of cloud base height from 24 CSCA airfields to dissect the past 67 years of summer stratus variability by site, subregion, altitude, and time of day. We diagnose the drivers of trends in, and interannual variability of, stratus cloud occurrence. Our findings are relevant to the densely populated and ecologically diverse CSCA region and a broader discussion of the future of subtropical marine clouds globally.

2. Methods

We evaluated annual records of summer stratus cloud frequency and base height during 1948–2014 using hourly measurements of cloud base height collected at 24 CSCA airfields (listed in Table S1 in the supporting information). Following *Schwartz et al.* [2014], we considered summer to be May–September, stratus clouds to have cloud bases at or below 1000 m above sea level (masl), and only hours 07:00, 10:00, 13:00, and 16:00 Pacific Standard Time to minimize missing observations. CSCA airfields (Figure 1) are clustered into four subregions: Santa Barbara (SB), Los Angeles (LA), San Diego (SD), and Islands. We calculated subregional records of stratus frequency by first standardizing each airfield's stratus-frequency record (converted to *z* scores) relative to the common period of 1973–2014 and then averaging across airfields (Figure 1b). For trend analysis of the subregional records, we added back in the average of the means and variances of the individual airfield time series within each subregion.

We also developed stratus-frequency records for lower altitude classes: the lowest 25%, 50%, 75% of stratus clouds. Each airfield has a unique upper bound for each height class, determined from the 25th, 50th, and 75th percentiles of stratus cloud base heights during May–September 1973–2014 (Table S2). We refer to the lowest 25% of stratus at each airfield as "fog." Following *Johnstone and Dawson* [2010], our definition is chosen because

the lowest 25% of stratus clouds are always low enough (generally <350 masl) to intersect with the coastal mountains that ring CSCA.

We evaluated airfield-specific and subregional trends in stratus frequency and base height. We determined trends using linear regression and statistical significance when Spearman's Rho and Kendall's Tau tests both indicate >95% confidence. Trends in stratus frequency are expressed as percent relative change per decade during the observation period. For clear distinction from relative trends, we refer to absolute stratus frequencies as fractions. We related trends in stratus frequency and cloud base height to changes in temperature and nearby urban area. Changes in urban area (ΔUrban) are considered within a 10 km radius of each airfield and calculated as the fraction of urban area in 2011 minus that in 1950. Urban areas for 2011 come from the latest version of the National Land Cover Database [*Jin et al.,* 2013]. Urban areas for 1950 are derived from census data [*Hammer et al.,* 2004] following *Syphard et al.* [2011]. See supporting information text for more information on land cover data. All significance and confidence intervals reflect uncertainty caused by reductions in effective sample size due to spatial or temporal autocorrelation [*Dawdy and Matalas*, 1964]. Spatial autocorrelation was calculated as the Moran's I coefficient [*Cliff and Ord*, 1981]. Confidence bounds around regression lines are expanded using variance inflation to account for uncertainty due to autocorrelation [*Wilks*, 2011].

We also evaluated interannual correlation between CSCA regional stratus records and other climate variables. The CSCA regional stratus record was calculated as the average of the SB, LA, and SD subregional records. The Islands subregion was excluded because our primary interest was in the highly populated, mainland CSCA. Linear trends were removed prior to correlation analyses to exclude common but potentially unrelated trends.

Throughout this article, we use Monte Carlo simulation to account for potential errors caused by measurement uncertainties and missing data. Briefly, each analysis was repeated 1000 times while continuously perturbing the data sets by adding random errors within known or assumed measurement uncertainties. All correlation significance values and regression confidence intervals are representative of at least 95% of the Monte Carlo simulation members and therefore account for measurement uncertainties. See supporting information text for more details about uncertainty characterization.

3. Results and Discussion

3.1. Dissection of CSCA Stratus Variability

Figure 1 shows subregional time series of May–September standardized stratus frequency during 1948–2014. Correlation is strongest among mainland subregions ($r = 0.73$–0.89) and weaker within the Islands subregion ($r = 0.58$–0.77). Within subregions, airfield-specific records generally correlate well ($r > 0.75$). Despite strong interannual covariability among airfields and subregions, there are substantial differences among long-term trends. Regional and airfield-specific trends are provided in Table S3. During 1948–2014, stratus frequency significantly declined by 23% in the LA subregion, supported by declines at all 11 LA airfields. Stratus declines were nearly ubiquitous in SD but only significant at three of eight airfields. Stratus frequency did not decline in the SB or Islands subregions.

Figure 2 (left column) shows subregional records of stratus frequency within two altitude classes. Blue represents the lowest 25% of stratus clouds (fog), and beige represents the remaining 75%. The 23% decline in LA stratus frequency since 1948 is largely driven by a 63% reduction in fog frequency. SD airfields also experienced fog reductions. Fog frequency did not change significantly in SB and increased significantly in the Islands subregion due to a substantial increase at San Nicolas Island (Table S3). These general differences among subregional trends in fog frequency were consistent for all individual summer months.

The trends described above were generally most pronounced in the early morning, when stratus, especially fog, is most common. Although nighttime hours are not included due to observational inconsistencies, airfield records with adequate data indicate that 07:00 trends are generally representative of nighttime hours, if not a bit weaker (Figure S1). Figure 2 (right column) represents stratus frequency at 07:00 only. These records indicate a significant reduction of 07:00 fog frequency in LA by 64% and also reduced fog at all airfields in SD (Table S4). The 07:00 fog frequency in the Islands subregion increased significantly, largely due to San Nicolas Island (Table S4). The significant increase in fog in the Islands subregion was entirely compensated

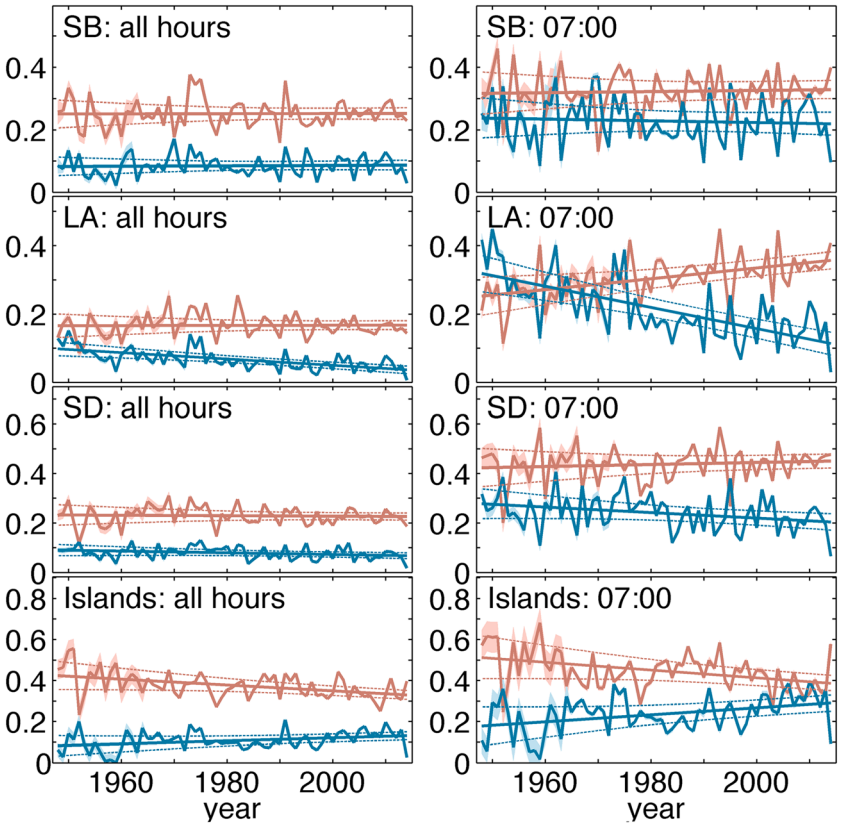

Figure 2. Subregional stratus frequency for the lowest 25% (blue) and remaining 75% (beige) of stratus clouds. (left column) All hours (07:00, 10:00, 13:00, and 16:00). (right column) 07:00 only. Shaded areas represent 95% confidence intervals. Bold straight lines indicate linear trends, and thin lines bounding the trend line represent 95% confidence bounds for trends.

by significant decreases in upper 75% stratus (Figure 2). In the LA and SD subregions, upper 75% stratus frequency at 07:00 increased but not enough to fully compensate for the reduced fog frequency. Opposing trends among low and high stratus clouds indicate that cloud base heights have ascended in LA (and SD to a lesser extent) and descended over the Islands. Stratus cloud base heights at 07:00 increased at nearly all airfields in the urbanized LA and SD subregions (the average trend in LA was 12.7 m/decade).

3.2. Urban Warming Effects

Previous studies noted a substantial decline in the frequency of low-visibility fog events (visibility $<$400 m) at two LA airfields since 1950 [*LaDochy*, 2005; *LaDochy and Witiw*, 2012; *Witiw and LaDochy*, 2008]. Like these studies, we hypothesize that declining fog frequency in parts of CSCA has been associated with urban warming trends. The mechanism underlying this hypothesis is that urban surfaces exhibit reduced evapotranspiration and enhanced nighttime reradiation of energy due to prolonged storage of heat absorbed during the day, creating a surface warming forcing that most strongly affects daily minimum temperatures (T_{min}) [*Grimmond and Oke*, 1999; *Oke*, 1982]. Increased T_{min} positively forces the near-surface dew point depression (DPD = air temperature minus dew point temperature), causing the condensation level (CL) in the atmosphere to rise [e.g., *Bolton*, 1980], thus leading to increased cloud base height and reduced fog frequency. The close relationship between DPD and cloud base height is exemplified by a strong and positive spatial correlation between mean May–September 07:00 DPD and stratus cloud base heights during 2000–2014 among CSCA airfields ($r = 0.89$, $p < 0.005$; Figure S2).

Although long-term DPD records are too limited for evaluation of trends throughout CSCA [*Brown and DeGaetano*, 2013], we gain insights about the relationship between urbanization, warming, and stratus cloud response from Figure 3. Among the 24 CSCA airfields with adequate data, post-1948 linear trends in May–September daily minimum temperature (ΔT_{min}) were significantly and positively correlated

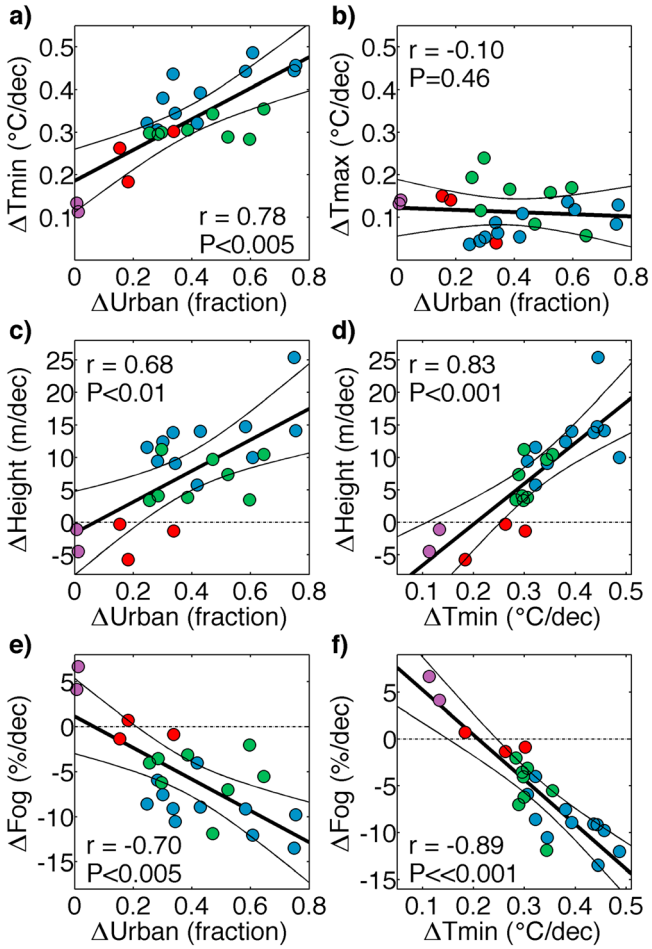

Figure 3. (a–f) Airfield-specific relationships between changes in temperature, urban cover, 07:00 stratus cloud base height, and 07:00 fog frequency. Each dot represents one of 24 CSCA airfields, and dot colors indicate subregion (red: SB, blue: LA, green: SD, and purple: Islands). Bold black lines: regression lines. Correlation significance values (*P* values) and 95% confidence intervals around regression lines reflect uncertainties due to spatial autocorrelation and measurement errors.

with ΔUrban ($r = 0.78$, $P < 0.005$), where heavy urbanization corresponded with approximately twice as much warming as light urbanization (Figure 3a). Trends in daily maximum temperature (ΔT_{max}) were not as strong and were unrelated to ΔUrban (Figure 3b).

Interpretation of the ΔUrban effect on ΔT_{min} is confounded because both variables are positively and significantly correlated with distance from coast ($r > 0.70$, $P < 0.005$; Figures S3a and S3b). This is expected because, given our consideration of urbanization within a radius of 10 km, airfields near the ocean have less available land area for urbanization. Preferential warming inland is also a robust feature of regional climate projections [e.g., *Walton et al.,* 2015], so it may be argued that the correlation between ΔUrban and ΔT_{min} is not causal. However, the positive correlation between ΔT_{min} and ΔUrban is still significant after distance from coast is accounted for ($r = 0.49$, $P < 0.05$; Figure S3c). In reality, ΔT_{min} has likely been influenced by both distance from coast and ΔUrban. While we cannot completely distinguish the two factors here, the interpretation of the importance of ΔUrban is consistent with prior studies in California [*Cayan and Douglas*, 1984; *LaDochy et al.,* 2007], and the exclusively positive relationship with ΔT_{min} (as opposed to ΔT_{max}) is consistent with the classic urban heat island effect [e.g., *Oke*, 1982]. Interestingly, the urban relationship with ΔT_{min} strengthens if absolute urban area in 2011 is considered rather than ΔUrban ($r = 0.88$, $P << 0.001$ and $r = 0.70$, $P < 0.005$ after distance from coast is accounted for; Figures S4a and S4b). These increases in correlation are statistically insignificant but suggest that areas urbanized prior to 1950 (not only areas urbanized after 1950) experienced elevated post-1950 increases in T_{min} due to intensification of urban processes such as energy consumption [e.g., *Böhm*, 1998; *McCarthy et al.,* 2010] and, possibly, enhanced temperature sensitivity to greenhouse forcing.

Among the 24 airfields, we find positive relationships between trends in 07:00 stratus cloud base height (ΔHeight) and both ΔUrban ($r = 0.68$, $P < 0.01$, Figure 3c) and ΔT_{min} ($r = 0.83$, $P < 0.001$, Figure 3d). Correspondingly, trends in fog frequency (ΔFog) correlate negatively with ΔUrban ($r = -0.70$, $P < 0.005$) and ΔT_{min} ($r = -0.89$, $P << 0.001$) (Figures 3e and 3f). As was the case for ΔT_{min}, the urban correlations with ΔHeight and ΔFog strengthen when absolute urban area in 2011 is considered ($r = 0.77$, $P < 0.001$ and $r = -0.85$, $P << 0.001$, respectively; Figures S4c and S4cd). Results are nearly identical if ΔFog is evaluated as absolute rather than relative and are also not substantially affected if trends are recalculated for only the common period 1973–2014. The general results were also consistent when ΔUrban was calculated within alternative radii (e.g., 5 km or 15 km).

The statistical relationships in Figure 3 implicate night and early morning warming as the primary driver of decreasing fog frequency in the most urbanized parts of LA and SD. This warming appears to be due to a combination of an urban heat island effect and a coast-to-inland warming gradient. Areas with the greatest reductions in fog frequency also have tended to experience reductions in overall stratus frequency during daytime hours (Table S3), likely affecting the solar radiation budget at the surface. Increased insolation may initiate a positive feedback by promoting further stratus reductions via daytime surface warming [e.g., *Rochetin et al.,* 2014]. This feedback may be exacerbated by warming-induced weakening of the temperature inversion [e.g., *Bornstein*, 1968], which we show next to be a dominant driver of stratus cloudiness.

3.3. Causes of Interannual Variability

To better understand coupling between CSCA stratus clouds and large-scale climate, we investigate the drivers of interannual variability. We consider low and high stratus clouds separately, defining low stratus (not to be mistaken with fog) as the lowest 75% of stratus clouds at each station and high stratus as the highest 25% of stratus clouds. We make this distinction because detrended stratus records for the three lowest height quartiles correlate positively with each other, and the records for the lowest two quartiles correlate negatively (insignificantly) with the record for the highest quartile.

Prior work indicates that subtropical stratus variability in and near CSCA, and also in subtropical stratocumulus regions globally, is strongly influenced by characteristics of the temperature inversion layer overlying the MBL [*Iacobellis and Cayan*, 2013; *Klein et al.,* 1995; *Muñoz et al.,* 2011; *Qu et al.,* 2014; *Wood and Bretherton*, 2006]. To investigate inversion relationships with stratus, we evaluate the radiosonde temperature record for the atmospheric profile at San Diego-Miramar Naval Air Station (NKX). Figure 4a shows the mean May–September atmospheric temperature profile. Figure 4b shows how the CSCA regional low- and high-stratus records correlate with temperature records throughout the profile. Low stratus correlates negatively with near-surface temperature. High stratus does not correlate with surface temperature but instead correlates negatively with temperature above the MBL.

The mechanism linking cold SSTs to low stratus appears to be primarily via the influence of SSTs on the strength of the atmospheric temperature inversion. Inversion strength is defined as the temperature difference between the top and bottom of the inversion layer (Figure 4a), and a relatively strong inversion reinforces atmospheric stability above the MBL [*Klein and Hartmann*, 1993; *Klein et al.,* 1995; *Qu et al.,* 2014; *Wood and Bretherton*, 2006]. Figure 4c indicates that the frequency of CSCA low stratus occurrence correlates strongly with inversion strength at NKX during 1960–2014 ($r = 0.78$, $P \ll 0.001$). Correlation is much stronger with inversion-base temperature (T_{base}; $r = -0.51$, $P \ll 0.001$) than with inversion-top temperature (T_{top}; $r = 0.05$, $P > 0.05$). However, T_{top} and T_{base} are positively correlated with each other ($r = 0.72$, $P \ll 0.001$), and correlation between low stratus and T_{top} increases to 0.70 ($P \ll 0.001$) after correlation with T_{base} is removed from both records, highlighting the importance of both a cold surface and a relatively warm free troposphere in promoting low stratus occurrence.

Variability in high stratus is strongly and positively associated with the inversion-layer height. An inversion-height metric that correlates particularly strongly with the high-stratus record is the percent of May–September days when NKX inversion-base height is at or above 800 masl ($r = 0.82$, $P \ll 0.001$; Figure 4d). Shown in Figure 4e, correlation with reanalysis upper atmospheric data for 1979–2014 [*Rienecker et al.,* 2011] suggests that high-stratus conditions correspond with weak synoptic frontal activity that reduces subsidence, cools the free troposphere, promotes convection within the MBL, and lifts the inversion layer. Although the high-stratus regime is more characteristic of autumn-spring [e.g., *Lin et al.,* 2009], relatively rare high stratus events during summer are important periodic regulators of insolation and temperature over land because these clouds tend to penetrate inland [*Iacobellis and Cayan*, 2013] and persist throughout the day.

Figure 4f shows correlation between frequency of the more common low stratus clouds and near-surface (surface to 950 hPa) temperature and wind velocity. Low stratus is most strongly associated with the local wind-driven coastal upwelling regime near CSCA and Baja California. An additional cause of the disproportionately strong correlation with near-surface temperature is the negative forcing that stratus clouds themselves impose on temperature within the MBL via shading [e.g., *Betts and Ridgway*, 1989]. Low stratus clouds are therefore self-promoting in that they help to strengthen the overlying temperature inversion. Although reanalysis and GCM data are too coarse to represent the temperature

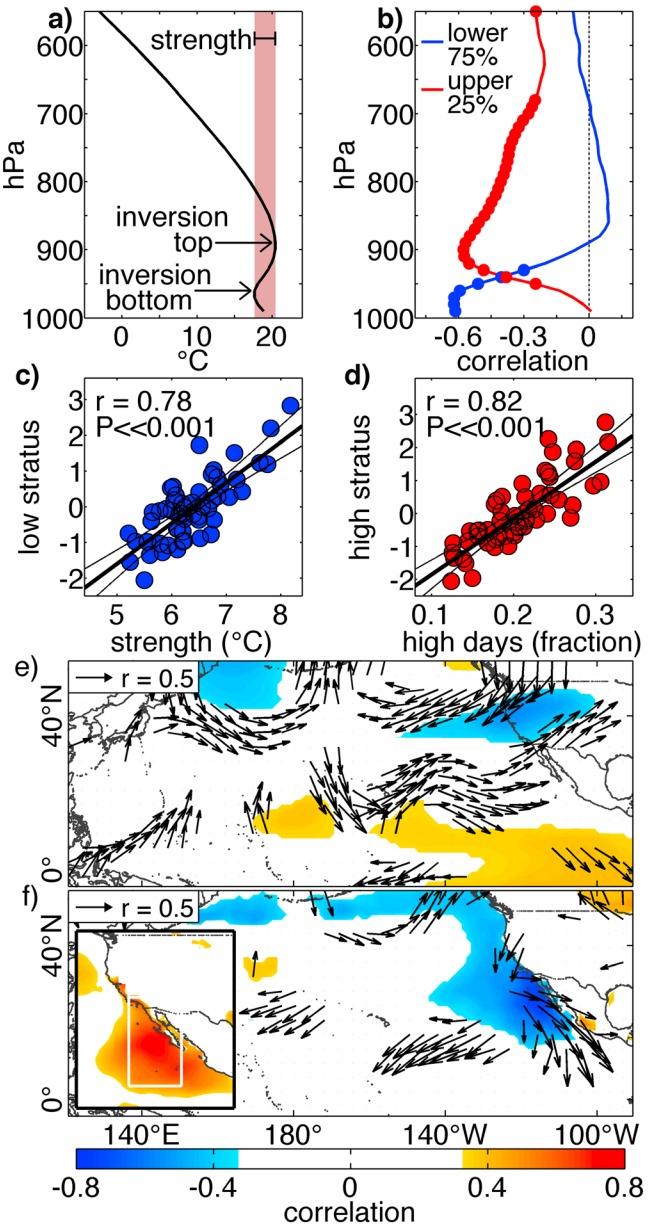

Figure 4. Drivers of interannual stratus variability. (a) Mean May–September temperature profile at San Diego-Miramar (NKX). (b) Correlation between NKX profile temperature and records of (blue) low and (red) high CSCA stratus frequency (dots: $P < 0.05$). Scatterplots of CSCA (c) low stratus versus NKX inversion strength and (d) CSCA high stratus versus fraction of days when inversion bottom ≥800 masl for 1960–2014. (e) Correlation map: CSCA high-stratus record versus upper tropospheric (500 to 200 hPa) temperature (background) and wind velocity (arrow vectors). (f) Correlation map: CSCA low stratus record versus near-surface (surface to 950 hPa) temperature and wind velocity. Inset in Figure 4f: CSCA low stratus record versus LTS. Lengths and directions of the arrow vectors in Figures 4e and 4f indicate correlation with zonal (west to east) and meridional (south to north) components of wind velocity. Correlation maps represent 1979–2014. Only significant correlations ($P < 0.05$) are shown. Correlation significance values and 95% confidence intervals around regression lines reflect uncertainties due to temporal autocorrelation and measurement errors. All time series were detrended prior to analysis.

inversion directly, an estimate of lower tropospheric stability (LTS) is the difference between potential temperature (θ) above the MBL (850 hPa) and at the surface [e.g., *Iacobellis et al.*, 2009]. Figure 4f inset indicates generally stronger correlation with LTS than with low-level temperature. Correlation between CSCA low stratus and LTS within the white box in the Figure 4f inset is $r = 0.75$ ($P \ll 0.001$), similar to correlation with NKX inversion strength during the same time period ($r = 0.73$, $P \ll 0.001$).

Importantly, the effects of inversion strength and LTS on low stratus may appear artificially suppressed by the confounding effects of subsidence. Subsidence, not only promotes stability across the MBL top by warming, favoring low stratus, but also has an opposing effect by promoting a shallower MBL, narrowing the vertical space between the MBL top and the CL [*Myers and Norris*, 2013]. This is supported in our study. The CSCA low stratus record correlates positively with subsidence over much of the northeast Pacific, but correlations are negative to neutral locally, particularly after correlations with LTS are removed from stratus and subsidence records (Figures S5a and S5b). This suggests that the vertical distance between the CL and MBL top is an important secondary factor influencing low stratus occurrence because it dictates cloud layer thickness (CLT). We estimate interannual variability in CLT for 1960–2014 as the difference between detrended, standardized time series of inversion-base height at NKX, and average stratus cloud base height at the CSCA airfields. After correlations with NKX inversion strength are removed, CLT correlates positively and significantly ($r = 0.57$, $P \ll 0.001$) with the CSCA low stratus record (Figure S5c). Inclusion of CLT with NKX inversion strength in a multiple regression increases correlation with the 1960–2014 CSCA low stratus record from $r = 0.78$ to $r = 0.86$ ($P \ll 0.001$; Figure S5d).

4. Conclusions

Fog occurrence has greatly declined since the midtwentieth century throughout the LA subregion. Fog reductions are due to increasing stratus cloud base heights, caused by nighttime increases in surface temperature and DPD. Rates of nighttime warming, cloud base lifting, and fog reductions are all strongly correlated with the fraction of surrounding area that has been urbanized. The fact that these cooccurring trends are confined to night and early morning implicates enhanced nighttime long-wave emission from warm urban surfaces as a primary driver of increased cloud base heights. Warming-driven increases in cloud base height are consistent with prior modeling efforts for coastal Northern California [*O'Brien*, 2011]. Increased cloud base heights have been accompanied by decreases in total stratus frequency throughout much of LA and parts of SD, suggesting an effective squeezing out of stratus clouds due to increasingly limited vertical space between the CL and top of the MBL.

Atmospheric stability above the MBL is also important in dictating CSCA stratus frequency. Stability above the MBL has likely enhanced over the Islands subregion due to rapid warming above the MBL and the absence of a local SST trend (Figures S6a and S6b). Curiously, Islands stratus frequency did not increase as a result of enhanced stability. Instead, stratus cloud bases simply descended at the Islands airfields, potentially driven by a reduction in the local MBL depth and resultant increases in MBL specific humidity (reducing DPD). Future research is needed to determine why Islands cloud bases descended and whether these trends would have also occurred on the mainland coast in the absence of urbanization.

Subtropical stratus clouds are important regulators of Earth's energy balance and may initiate feedbacks with the large-scale climate system [e.g., *Bellomo et al.,* 2014b]. Understanding future stratus trends globally is difficult because the drivers of temporal variations appear to differ regionally and there is little consensus among GCMs regarding what these drivers are [*Bellomo et al.,* 2014a; *Qu et al.,* 2014; *Webb et al.*, 2013]. In the Northeast Pacific and greater CSCA region, GCMs converge upon intensification of upwelling [*Wang et al.*, 2015] and continued increases in stability above the MBL [*Webb et al.*, 2013, *Qu et al.*, 2014], but GCMs also project substantial increases in free-tropospheric specific humidity, which should inhibit stratus [*Klein et al.,* 1995; *Wood*, 2012; *Wood and Bretherton*, 2004], and are in disagreement regarding projected trends in regional subsidence, which may promote stratus [*Sandu and Stevens*, 2011] or inhibit it [*Myers and Norris*, 2013]. See Figure S6c for CMIP5 projections of LTS, specific humidity, and vertical velocity over subtropical Northeast Pacific.

In CSCA, the complex effects of large-scale climate change on stratus clouds will be superimposed upon the effects of urban warming. Since the mid-1900s, early morning stratus cloud base heights ascended at most airfields evaluated in CSCA, with the largest increases in the LA subregion. Projections of continued background warming in combination with continued population growth [*Syphard et al.,* 2005, 2011] suggest that urbanization and rising cloud base heights will continue to occur throughout much of CSCA in the coming decades, corresponding to changes in the spatial distribution of fog on coastal mountainsides. In the absence of an equal increase in MBL depth, rising cloud base heights will increasingly correspond to reductions in summer cloudiness. Reduced daytime cloudiness would promote a positive feedback by reducing daytime cloud shading, potentially counteracting cooling effects of an enhanced sea breeze [*Lebassi et al.,* 2009]. Reduced fog and stratus frequency may improve transportation safety and potential for solar energy capture but intensify water and energy demand through increased solar radiation and decreased deposition of fog water and dew. The diverse and flammable ecosystems of the coastal mountains that ring the CSCA urban lowlands rely on regular inundation and shading by summer stratus clouds for drought regulation and would be particularly affected by rising cloud base heights and reduced stratus frequency.

Acknowledgments

Airfield data are from the U.S. Surface Airways Hourly Data Set, provided by the National Climate Data Center (ftp.ncdc.noaa.gov/pub/data/noaa/). Monthly T_{min} and T_{max} data are from PRISM (Oregon State University, www.prism.nacse.org). Radiosonde data are from www.esrl.noaa.gov/raobs. Land cover data come from www.mrlc.gov/nlcd2011.php, http://glcf.umd.edu, and http://silvis.forest.wisc.edu/maps/housing/pbg_1940_2030. Climate reanalysis data are from NASA's MERRA product (disc.sci.gsfc.nasa.gov/daac-bin/DataHoldings.pl). Research was supported by the Lamont-Doherty Earth Observatory of Columbia University and NSF award EASM2: Linking Near-term Future Changes in Weather and Hydroclimate in Western North America to Adaptation for Ecosystem and Water Management. Thanks for helpful comments from S.A. Baguskas, K. Bellomo, D. Cayan, K.D. Clarke, E.R. Cook, C. Gautier, A. Gershunov, P. Gentine, J.E. Smerdon, and E. Waller.

The Editor thanks two anonymous reviewers for their assistance in evaluating this paper.

References

Akbari, H., M. Pomerantz, and H. Taha (2001), Cool surfaces and shade trees to reduce energy use and improve air quality in urban areas, *Sol. Energy*, *70*(3), 295–310, doi:10.1016/S0038-092X(00)00089-X.

Baguskas, S. A., S. H. Peterson, B. Bookhagen, and C. J. Still (2014), Evaluating spatial patterns of drought-induced tree mortality in a coastal California pine forest, *For. Ecol. Manage.*, *315*, 43–53, doi:10.1016/j.foreco.2013.12.020.

Bellomo, K., A. C. Clement, J. R. Norris, and B. J. Soden (2014a), Observational and model estimates of cloud amount feedback over the Indian and Pacific Oceans, *J. Clim.*, *27*(2), 925–940, doi:10.1175/JCLI-D-13-00165.1.

Bellomo, K., A. Clement, T. Mauritsen, G. Rädel, and B. Stevens (2014b), Simulating the role of subtropical stratocumulus clouds in driving Pacific climate variability, *J. Clim.*, *27*(13), 5119–5131, doi:10.1175/JCLI-D-13-00548.1.

Betts, A. K., and W. Ridgway (1989), Climatic equilibrium of the atmospheric convective boundary layer over a tropical ocean, *J. Atmos. Sci.*, *46*(17), 2621–2641, doi:10.1175/1520-0469(1989)046<2621:CEOTAC>2.0.CO%3B2.

Böhm, R. (1998), Urban bias in temperature time series—A case study for the city of Vienna, Austria, *Clim. Change*, *38*(1), 113–128, doi:10.1023/A:1005338514333.

Bolton, D. (1980), The computation of equivalent potential temperature, *Mon. Weather Rev.*, *108*(7), 1046–1053, doi:10.1175/1520-0493(1980)108<1046:TCOEPT>2.0.CO%3B2.

Bornstein, R. D. (1968), Observations of the urban heat island effect in New York City, *J. Appl. Meteorol.*, *7*(4), 575–582, doi:10.1175/1520-0450(1968)007<0575:OOTUHI>2.0.CO;2.

Brown, P. J., and A. T. DeGaetano (2013), Trends in US surface humidity, 1930–2010, *J. Appl. Meteorol. Climatol.*, *52*(1), 147–163, doi:10.1175/JAMC-D-12-035.1.

Carbone, M. S., A. P. Williams, A. R. Ambrose, C. M. Boot, E. S. Bradley, T. E. Dawson, S. M. Schaeffer, J. P. Schimel, and C. J. Still (2013), Cloud shading and fog drip influence the metabolism of a coastal pine ecosystem, *Global Change Biol.*, *19*(2), 484–497, doi:10.1111/gcb.12054.

Cayan, D. R., and A. V. Douglas (1984), Urban influences on surface temperatures in the southwestern United States during recent decades, *J. Clim. Appl. Meteorol.*, *23*(11), 1520–1530, doi:10.1175/1520-0450(1984)023<1520:UIOSTI>2.0.CO;2.

Clement, A. C., R. Burgman, and J. R. Norris (2009), Observational and model evidence for positive low-level cloud feedback, *Science*, *325*(5939), 460–464, doi:10.1126/science.1171255.

Cliff, A. D., and J. K. Ord (1981), Spatial and temporal analysis: Autocorrelation in space and time, in *Quantitative Geography: A British View*, edited by E. N. Wrigley and R. J. Bennett, pp. 104–110, Routledge and Kegan Paul, London, U. K.

Corbin, J. D., M. A. Thomsen, T. E. Dawson, and C. M. D'Antonio (2005), Summer water use by California coastal prairie grasses: Fog, drought, and community composition, *Oecologia*, *145*(4), 511–521, doi:10.1007/s00442-005-0152-y.

Dawdy, D. R., and N. C. Matalas (1964), Statistical and probability analysis of hydrologic data, part III: Analysis of variance, covariance and time series, in *Handbook of Applied Hydrology, A Compendium of Water-Resources Technology*, edited by V. T. Chow, pp. 8.68–8.90, McGraw-Hill Book Company, New York.

Dawson, T. E. (1998), Fog in the California redwood forest: Ecosystem inputs and use by plants, *Oecologia*, *117*(4), 476–485, doi:10.1007/s004420050683.

Fischer, D. T., C. J. Still, and A. P. Williams (2009), Significance of summer fog and overcast for drought stress and ecological functioning of coastal California endemic plant species, *J. Biogeogr.*, *36*(4), 783–799, doi:10.1111/j.1365-2699.2008.02025.x.

Grimmond, C. S. B., and T. R. Oke (1999), Heat storage in urban areas: Local-scale observations and evaluation of a simple model, *J. Appl. Meteorol.*, *38*(7), 922–940, doi:10.1175/1520-0450(1999)038<0922:HSIUAL>2.0.CO%3B2.

Hammer, R. B., S. I. Stewart, R. L. Winkler, V. C. Radeloff, and P. R. Voss (2004), Characterizing dynamic spatial and temporal residential density patterns from 1940–1990 across the North Central United States, *Landscape Urban Plann.*, *69*(2), 183–199, doi:10.1016/j.landurbplan.2003.08.011.

Hartmann, D. L., M. E. Ockert-Bell, and M. L. Michelsen (1992), The effect of cloud type on Earth's energy balance: Global analysis, *J. Clim.*, *5*(11), 1281–1304, doi:10.1175/1520-0442(1992)005<1281:TEOCTO>2.0.CO;2.

Huang, X.-Y., A. Hall, and J. Teixeira (2013), Evaluation of WRF PBL parameterizations for marine boundary layer clouds: Cumulus and stratocumulus, *Mon. Weather Rev.*, *141*(7), 2265–2271, doi:10.1175/MWR-D-12-00292.1.

Iacobellis, S. F., and D. R. Cayan (2013), The variability of California summertime marine stratus: Impacts on surface air temperatures, *J. Geophys. Res. Atmos.*, *118*, 9105–9122, doi:10.1002/jgrd.50652.

Iacobellis, S. F., J. R. Norris, M. Knamitsu, M. Tyree, and D. C. Cayan (2009), Climate variability and California low-level temperature inversions, *Rep. CEC-500-2009-020-F*, Calif. Clim. Change Cent., Sacramento.

Jin, S., L. Yang, P. Danielson, C. Homer, J. Fry, and G. Xian (2013), A comprehensive change detection method for updating the national land cover database to circa 2011, *Remote Sens. Environ.*, *132*, 159–175, doi:10.1016/j.rse.2013.01.012.

Johnstone, J. A., and T. E. Dawson (2010), Climatic context and ecological implications of summer fog decline in the coast redwood region, *Proc. Natl. Acad. Sci. U.S.A.*, *107*(10), 4533–4538, doi:10.1073/pnas.0915062107.

Klein, S. A., and D. L. Hartmann (1993), The seasonal cycle of low stratiform clouds, *J. Clim.*, *6*(8), 1587–1606, doi:10.1175/1520-0442(1993)006<1587:TSCOLS>2.0.CO;2.

Klein, S. A., D. L. Hartmann, and J. R. Norris (1995), On the relationships among low-cloud structure, sea surface temperature, and atmospheric circulation in the summertime northeast Pacific, *J. Clim.*, *8*(5), 1140–1155, doi:10.1175/1520-0442(1995)008<1140:OTRALC>2.0.CO%3B2.

Knowlton, K., M. Rotkin-Ellman, G. King, H. G. Margolis, D. Smith, G. Solomon, R. Trent, and P. English (2009), The 2006 California heat wave: Impacts on hospitalizations and emergency department visits, *Environ. Health Perspect.*, *117*(1), 61–67, doi:10.1289/ehp.11594.

LaDochy, S. (2005), The disappearance of dense fog in Los Angeles: Another urban impact?, *Phys. Geogr.*, *26*(3), 177–191, doi:10.2747/0272-3646.26.3.177.

LaDochy, S., and M. Witiw (2012), The continued reduction in dense fog in the Southern California region: Possible causes, *Pure Appl. Geophys.*, *169*(5–6), 1157–1163, doi:10.1007/s00024-011-0366-3.

LaDochy, S., R. Medina, and W. Patzert (2007), Recent California climate variability: Spatial and temporal patterns in temperature trends, *Clim. Res.*, *33*(2), 159–169, doi:10.3354/cr033159.

Lauer, A., K. Hamilton, Y. Wang, V. T. J. Phillips, and R. Bennartz (2010), The impact of global warming on marine boundary layer clouds over the eastern Pacific—A regional model study, *J. Clim.*, *23*(21), 5844–5863, doi:10.1175/2010JCLI3666.1.

Lebassi, B., J. Gonzalez, D. Fabris, E. Maurer, N. Miller, C. Milesi, P. Switzer, and R. Bornstein (2009), Observed 1970–2005 cooling of summer daytime temperatures in coastal California, *J. Clim.*, *22*(13), 3558–3573, doi:10.1175/2008JCLI2111.1.

Lin, W., M. Zhang, and N. G. Loeb (2009), Seasonal variation of the physical properties of marine boundary layer clouds off the California coast, *J. Clim.*, *22*(10), 2624–2638, doi:10.1175/2008JCLI2478.1.

McCarthy, M. P., M. J. Best, and R. A. Betts (2010), Climate change in cities due to global warming and urban effects, *Geophys. Res. Lett.*, *37*, L09705, doi:10.1029/2010GL042845.

Muñoz, R., R. Zamora, and J. Rutllant (2011), The coastal boundary layer at the eastern margin of the southeast Pacific (23.4°S, 70.4°W): Cloudiness-conditioned climatology, *J. Clim.*, *24*(4), 1013–1033, doi:10.1175/2010JCLI3714.1.

Myers, T. A., and J. R. Norris (2013), Observational evidence that enhanced subsidence reduces subtropical marine boundary layer cloudiness, *J. Clim.*, *26*(19), 7507–7524, doi:10.1175/JCLI-D-12-00736.1.

O'Brien, T. A. (2011), The recent past and possible future decline of California coastal fog, Doctoral thesis, 193 pp, Univ. of California, Santa Cruz, Calif.

O'Brien, T. A., L. C. Sloan, P. Y. Chuang, I. C. Faloona, and J. A. Johnstone (2013), Multidecadal simulation of coastal fog with a regional climate model, *Clim. Dyn.*, *40*(11–12), 2801–2812, doi:10.1007/s00382-012-1486-x.

Oke, T. R. (1982), The energetic basis of the urban heat island, *Q. J. R. Meteorol. Soc.*, *108*(455), 1–24, doi:10.1002/qj.49710845502.

Qu, X., A. Hall, S. A. Klein, and P. M. Caldwell (2014), On the spread of changes in marine low cloud cover in climate model simulations of the 21st century, *Clim. Dyn.*, *42*(9–10), 2603–2626, doi:10.1007/s00382-013-1945-z.

Rienecker, N. M., et al. (2011), MERRA—NASA's Modern-Era Retrospective Analysis for Research and Applications, *J. Clim.*, *24*(14), 3624–3648, doi:10.1175/jcli-d-11-00015.1.

Rochetin, N., B. R. Lintner, K. L. Findell, A. H. Sobel, and P. Gentine (2014), Radiative convective equilibrium over a land surface, *J. Clim.*, *27*(23), 8611–8629, doi:10.1175/JCLI-D-13-00654.1.

Sandu, I., and B. Stevens (2011), On the factors modulating the stratocumulus to cumulus transitions, *J. Atmos. Sci.*, *68*(9), 1865–1881, doi:10.1175/2011JAS3614.1.

Sawaske, S. R., and D. L. Freyberg (2014), Fog, fog drip, and streamflow in the Santa Cruz Mountains of the California Coast Range, *Ecohydrology*, doi:10.1002/eco.1537.

Schwartz, R. E., A. Gershunov, S. F. Iacobellis, and D. R. Cayan (2014), North American west coast summer low cloudiness: Broad scale variability associated with sea surface temperature, *Geophys. Res. Lett.*, *41*, 3307–3314, doi:10.1002/2014GL059825.

Soden, B. J., and G. A. Vecchi (2011), The vertical distribution of cloud feedback in coupled ocean-atmosphere models, *Geophys. Res. Lett.*, *38*, L12704, doi:10.1029/2011GL047632.

Syphard, A. D., K. C. Clarke, and J. F. Franklin (2005), Using a cellular automaton model to forecast the effects of urban growth on habitat pattern in Southern California, *Ecol. Complexity*, *2*(2), 185–203, doi:10.1016/j.ecocom.2004.11.003.

Syphard, A. D., K. C. Clarke, J. Franklin, H. M. Regan, and M. Mcginnis (2011), Forecasts of habitat loss and fragmentation due to urban growth are sensitive to source of input data, *J. Environ. Manage.*, *92*(7), 1882–1893, doi:10.1016/j.jenvman.2011.03.014.

Torregrosa, A., T. A. O'Brien, and I. C. Faloona (2014), Coastal fog, climate change, and the environment, *Eos Trans. AGU*, *95*(50), 473–474, doi:10.1002/2014EO500001.

Vasey, M. C., M. E. Loik, and V. T. Parker (2012), Influence of summer marine fog and low cloud stratus on water relations of evergreen woody shrubs (Arctostaphylos: Ericaceae) in the chaparral of central California, *Oecologia*, *170*(2), 325–337, doi:10.1007/s00442-012-2321-0.

Walton, D. B., F. Sun, A. Hall, and S. Capps (2015), A hybrid dynamical-statistical downscaling technique, part I: Development and validation of a technique, *J. Clim.*, in press.

Wang, D., T. C. Gouhier, B. A. Menge, and A. R. Ganguly (2015), Intensification and spatial homoginization of coastal upwelling under climate change, *Nature*, *518*, 390–394, doi:10.1038/nature14235.

Webb, M. J., C. A. Senior, D. M. H. Sexton, W. J. Ingram, K. D. Williams, M. A. Ringer, B. J. McAvaney, R. Colman, B. J. Soden, and R. Gudgel (2006), On the contribution of local feedback mechanisms to the range of climate sensitivity in two GCM ensembles, *Clim. Dyn.*, *27*(1), 17–38, doi:10.1007/s00382-006-0111-2.

Webb, M. J., F. H. Lambert, and J. M. Gregory (2013), Origins of differences in climate sensitivity, forcing and feedback in climate models, *Clim. Dyn.*, *40*(3–4), 677–707, doi:10.1007/s00382-012-1336-x.

Wilks, D. S. (2011), *Statistical Methods in the Atmospheric Sciences*, 3rd ed., pp. 676, Academic Press, Oxford, U. K.

Williams, A. P., C. J. Still, D. T. Fischer, and S. W. Leavitt (2008), The influence of summertime fog and overcast clouds on the growth of a coastal Californian pine: A tree-ring study, *Oecologia*, *156*(3), 601–611, doi:10.1007/s00442-008-1025-y.

Williams, A. P., et al. (2015), Correlations between components of the water balance and burned area reveal new insights for predicting fire activity in the southwest US, *Int. J. Wildland Fire*, *24*(1), 14–26, doi:10.1071/WF14023.

Witiw, M. R., and S. LaDochy (2008), Trends in fog frequencies in the Los Angeles Basin, *Atmos. Res.*, *87*(3), 293–300, doi:10.1016/j.atmosres.2007.11.010.

Wood, R. (2012), Stratocumulus clouds, *Mon. Weather Rev.*, *140*(8), 2373–2423, doi:10.1175/MWR-D-11-00121.1.

Wood, R., and C. S. Bretherton (2004), Boundary layer depth, entrainment, and decoupling in the cloud-capped subtropical and tropical marine boundary layer, *J. Clim.*, *17*(18), 3576–3588, doi:10.1175/1520-0442(2004)017<3576:BLDEAD>2.0.CO;2.

Wood, R., and C. S. Bretherton (2006), On the relationship between stratiform low cloud cover and lower-tropospheric stability, *J. Clim.*, *19*(24), 6425–6432, doi:10.1175/jcli3988.1.